Mitochondria Play a Central Role in Apoptosis Induced by α-Tocopheryl Succinate, an Agent with Antineoplastic Activity: Comparison with Receptor-Mediated Pro-Apoptotic Signaling†

Tobias Weber,‡ Helge Dalen,§ Ladislav Andera,|| Anne Nègre-Salvayre,⊥ Nathalie Augé,⊥ Martin Sticha,# Ana Lloret,£ Alexei Terman,⊗ Paul K. Witting,○ Masahiro Higuchi,▽ Magdalena Plasilova,+ Jan Zivny,@ Nina Gellert,‡ Christian Weber,‡,● and Jiri Neuzil*,‡,⊗

Institute for Prevention of Cardiovascular Diseases, Ludwig Maximilians University, Munich, Germany, Department of Pathology, The Gade Institute, University of Bergen, Norway, Institute of Molecular Genetics, Czech Academy of Sciences, Prague, Czech Republic, Biochemistry Department, Paul Sabatier University, Toulouse, France, Faculty of Science, Charles University, Prague, Czech Republic, Department of Physiology, University of Valencia, Spain, Division of Pathology II, Faculty of Health Sciences, University Hospital, Linköping, Sweden, Heart Research Institute, Sydney, NSW, Australia, Department of Neurology, Baylor College of Medicine, Houston, Texas, Institute of Hematology and Blood Transfusion and Department of Pathophysiology, Charles University First School of Medicine, Prague, Czech Republic, and Department of Cardiovascular Molecular Biology, University Hospital, Aachen, Germany

Received August 8, 2002; Revised Manuscript Received February 5, 2003

ABSTRACT: α-Tocopheryl succinate (α-TOS) is a semisynthetic vitamin E analogue with high pro-apoptotic and anti-neoplastic activity [Weber, T et al. (2002) *Clin. Cancer Res. 8*, 863−869]. Previous studies suggested that it acts through destabilization of subcellular organelles, including mitochondria, but compelling evidence is missing. Cells treated with α-TOS showed altered mitochondrial structure, generation of free radicals, activation of the sphingomyelin cycle, relocalization of cytochrome *c* and Smac/Diablo, and activation of multiple caspases. A pan-caspase inhibitor suppressed caspase-3 and -6 activation and phosphatidyl serine externalization, but not decrease of mitochondrial membrane potential or generation of radicals. For α-TOS, but not Fas or TRAIL, apoptosis was suppressed by caspase-9 inhibition, while TRAIL- and Fas-resistant cells overexpressing cFLIP or CrmA were susceptible to α-TOS. The central role of mitochondria was confirmed by resistance of mtDNA-deficient cells to α-TOS, by regulation of α-TOS apoptosis by Bcl-2 family members, and by anti-apoptotic activity of mitochondrially targeted radical scavengers. Co-treatment with α-TOS and anti-Fas IgM showed their cooperative effect, probably by signaling via different, convergent pathways. These data provide an insight into the molecular mechanism, by which α-TOS kills malignant cells, and advocate its testing as a potential anticancer agent or adjuvant.

Apoptosis is a form of cell suicide essential for tissue development and remodeling and is responsible for elimination of redundant and/or deleterious cells. Better understanding of the mechanism and regulation of apoptotic processes may provide an approach to new therapeutic strategies (*1*). Apoptosis is associated with characteristic morphological and biochemical changes and encompasses a complex system of effectors, which converge on the proteolytic system of caspases (*2*). These enzymes build up a cascade which operates in both drug- and receptor-induced apoptosis (*3*, *4*) and which can be dissected to the initiator caspases that transmit the early pro-apoptotic events, and the effector caspases cleaving the death substrate (*5*) leading to the irreversible stage of the cell death program (*2*).

An important subcellular organelle, whose destabilization precedes activation of caspases in some types of apoptosis, is the mitochondrium (*6*). Many apoptotic stimuli induce mitochondrial swelling, opening of the permeability transition pore, dissipation of the mitochondrial potential (*7*), and release of mitochondrial pro-apoptotic proteins, such as the apoptosis inducing factor (AIF) (*8*), cytochrome *c* (cyt *c*) (*9*, *10*), and Smac/Diablo (*11*, *12*). In many instances, this leads to the formation of the apoptosome, a complex

† This work was supported in part by the University of Linköping Grant 83081030 and the Dust Diseases Board Grant (J.N.), the Norwegian Research Council Grant 129557/310 (H.D.), the DFG Grants We-1913/2 and GK-438 (C.W.), Grant A505 3001 from the Grant Agency of the Czech Republic (L.A.), and the GACR 301/00/1061 and IGAMZ 6689-3 grants (J.Z. and M.P.).

* Corresponding author. Address: Heart Foundation Research Center, School of Health Sciences, Griffith University, Southport, 4726 Queensland, Australia. Fax: +61-7-555-28905. Phone: +61-7-555-29109. E-mail: jneuzil@hotmail.com.

‡ Ludwig Maximilians University.
§ University of Bergen.
|| Czech Academy of Sciences.
⊥ Paul Sabatier University.
Charles University.
£ University of Valencia.
⊗ University Hospital, Linköping.
○ Heart Research Institute.
▽ Baylor College of Medicine.
+ Institute of Hematology and Blood Transfusion, Charles University First School of Medicine.
@ Department of Pathophysiology, Charles University First School of Medicine.
● University Hospital, Aachen.

10.1021/bi020527j CCC: $25.00
Published on Web 03/22/2003

consisting of cyt *c*, Apaf-1, and pro-caspase-9, followed by dATP-dependent activation of caspase-9 (*13*), while AIF-dependent cell death signaling appears to bypass the caspase cascade (*8*). Smac/Diablo translocates to the cytosol, where it associates with and suppresses the activity of the inhibitor of apoptosis proteins (IAPs) (*11*, *12*). The initiator caspase-9 or -8 (the latter activated by pro-caspase-8 recruitment to the death domain-containing adaptor protein in receptor-mediated apoptosis (*14*)) activates the executioner caspase-3, -6, or -7 (*5*, *15*). Thus, in drug-induced apoptosis, activation of the executioner caspases largely involves mitochondrial destabilization (*5*, *15*). On the other hand, receptor-mediated apoptosis involves activation of the initiator caspase-8 that relays the pro-apoptotic signal directly to effector caspases or indirectly, for example, by cleaving the protein Bid to its pro-apoptotic form, also resulting in mitochondrial injury (*10*, *14*).

Various effector molecules, such as the Bcl-2 family proteins, regulate pro-apoptotic signaling pathways (*16*). Of these, Bcl-2 has been shown to suppress apoptosis by inhibiting destabilization of mitochondria and preventing release of pro-apoptotic factors (*17*, *18*). The anti-apoptotic activity of Bcl-2 is modulated by different mechanisms, including multiple protein kinases and proteases either sensitizing the protein for degradation (*18*, *19*) or regulating its mitochondrial membrane association (*20*, *21*). Effector caspases also cleave the anti-apoptotic Bcl-2 to a pro-apoptotic Bax-like protein, hence modulating cell death by feedback amplification (*22*).

We have recently shown that α-tocopheryl succinate (α-TOS), an esterified analogue of vitamin E (VE), induced apoptosis in Jurkat cells, and this process involved subcellular organelle destabilization and activation of caspase-3 (*23*, *24*). Analogues of vitamin E have been shown to induce cell death in other malignant cell lines (*25*−*27*). The last of these studies showed that Trolox, a water-soluble analogue of VE, synergized in cancer cell killing with 5-fluorouracil, thereby overcoming resistance to apoptosis in cancer cells with mutant p53 by upregulating the cell cycle inhibitor protein $p21^{Waf1/Cip1}$. We have reported that α-TOS is effective against colon cancer cells regardless their tumor-suppressor gene status and against colon cancer in vivo (*24*, *28*), and that it is largely selective for malignant cells (*26*).

To extend our understanding of the molecular mechanism of cell death triggered by α-TOS, we investigated the role of mitochondria in apoptosis induced by the VE analogue, and the associated up- and downstream events. Here we show that mitochondria play a central role in this process and that their destabilization involves formation of reactive oxygen species (ROS), release of cyt *c*, and activation of multiple caspases in lymphoma and epithelial cells. Our results support the emerging picture of VE succinate as an agent with a high therapeutic potential.

[1] Abbreviations: AIF, apoptosis-inducing factor; BFU-E, erythroid burst-forming units; CFU-GM, granulocyte-macrophage colony-forming units; cyt *c*, cytochrome *c*; DCDF, 2′,7′-dichlorodihydrofluorescein diacetate; DMPO, 5,5-dimethyl-1-pyrroline *N*-oxide; EGFP, enhanced green fluorescent protein; EPR, electron paramagnetic resonance; FACS, fluorescence-assisted cell sorting; IAP, inhibitor of apoptosis protein; JC-1, 5,5′,6,6′-tetrachloro-1,1′,3,3′-tetraethylbenzimido-azolyl-carbocyanino iodide; mito-Q, mitochondrially targeted coenzyme Q; mtDNA, mitochondrial DNA; NAC, *N*-acetylcysteine; ODN, oligodeoxynucleotide; PS, phosphatidyl serine; SM, sphingomyelin; α-TOH, α-tocopherol; α-TOS, α-tocopheryl succinate; TRAIL, tumor necrosis factor-related apoptosis-inducing ligand; VE, vitamin E.

MATERIAL AND METHODS

Cell Culture and Treatment. Human parental, Bcl-2-overexpressing (*17*), Fas-dominant negative (DN) (*29*) and CrmA-overexpressing Jurkat cells (*30*), and THP-1 cells were cultured in RPMI medium with 10% FCS. The murine leukemia NSF/N1.H7 parental cells and their vector, gain-of-function (S70E), and loss-of-function (S70A) Bcl-2 transfectants were grown in RPMI medium with 10% FCS and 10% conditioned media from the IL-3-secreting WEHI-3 cells (*20*, *31*). Ml-1a cells, the Ml-1a-derived mtDNA-deficient (ρ^0) C19 cells, and the revertant P2 cells were grown in complete RPMI medium with supplements as specified elsewhere (*32*). Wild-type MCF7 cells and their stable caspase-3 transfectants (MCF7-C3) (*33*) were grown in EMEM with 10% FCS. Fibroblasts deficient in mtDNA were prepared by long-term treatment of human fibroblasts (strain AG01516) with sublethal doses of EtBr and kept in the same medium as the Ml-1a cells.

For experiments, suspension cells were seeded at 0.5×10^6 per mL and adherent cells used at 70−90% confluence, unless specified otherwise. Cells were treated with α-TOS (Sigma), anti-Fas IgM (clone CH-11; Immunotech), or the recombinant human tumor necrosis factor-related apoptosis-inducing ligand (rhTRAIL, Apo2L) (*34*). In some experiments, cells were pre- or co-treated with the neutralizing anti-Fas IgG (Upstate Biotechnology), α-tocopherol (α-TOH) (D-α-tocopherol; Sigma), the mitochondrially targeted analogues of α-tocopherol (mito-E) (*35*) or ubiquinone-10 (mito-Q) (*36*), *N*-acetyl-L-cysteine (NAC), caspase inhibitors (all Calbiochem), or desipramine (Sigma).

Assessment of Apoptosis Markers. In most cases, apoptosis was assessed by annexin V-binding to phosphatidyl serine (PS) externalized early in the process of apoptosis. In brief, cells were resuspended in the binding buffer, incubated with FITC- or PE-conjugated annexin V (PharMingen) and analyzed by fluorescence-assisted cell sorting (FACS) (FACScan or BDH LSR; Becton Dickinson) (*37*).

Caspase activity was measured as published elsewhere (*37*). In brief, cells were lysed, the lysate mixed with the reaction buffer, and incubated with substrates for caspase-3, -6, or -9, Ac-DEVD-AMC, Ac-VEID-pNA, or Ac-LEHD-AMC (50 μM each), respectively. The intensity of fluorescence of the liberated 4-amino-7-methyl coumarin (AMC) was measured at $\lambda_{ex} = 380$ nm and $\lambda_{em} = 435$ nm for Ac-DEVD-AMC, and $\lambda_{ex} = 400$ nm and $\lambda_{em} = 505$ for Ac-LEHD-AMC, while absorbance at 405 nm of the liberated *p*-nitroaniline (pNA) was measured in the case of Ac-VEID-pNA.

Caspase-3 activation was assessed by FACS as follows. Fixed and permeabilized cells were incubated with an antibody against the active form of caspase-3 (PharMingen) followed by FITC-conjugated secondary IgG and analyzed by FACS.

Mitochondrial inner membrane potential ($\Delta\Psi_m$) was assessed by incubating cells with 10 μM 5,5′,6,6′-tetrachloro-1,1′,3,3′-tetraethylbenzimidoazolyl-carbocyanino iodide (JC-1; Molecular Probes) and their analysis by FACS.

Assessment of GSH and GSSG Levels and Analysis of Free Radical Generation. GSH concentration in cells was deter-

mined based on the level of GSSG and total glutathione, using the equation [GSH] = [total glutathione] − 2 × [GSSG] as described earlier (*38*). The protocol for measurement of cellular levels of GSSG was published previously (*39*).

Formation of ROS was assessed indirectly as published (*40*). In brief, cells were incubated with 5 μM 2′,7′-dichlorodihydrofluorescein diacetate (DCDF; Molecular Probes), and fluorescence intensity was assessed by FACS. The oxidation nonsensitive analogue of DCDF, carboxy-DCDF (Molecular Probes) was used to rule out other than oxidation-dependent changes in DCDF flurescence.

ROS generation was also assessed directly by electron paramagnetic resonance (EPR) spectroscopy using the radical trap 5,5-dimethyl-1-pyrroline *N*-oxide (DMPO; Sigma) purified prior to use (*41*). Spin trapping of radicals readily allows their detection at room temperature (*42*). Buffers were stored over Chelex-100 (BioRad) to remove transition metals. X-band spectra (293 or 77 K) were obtained with a Bruker EPR benchtop spectrometer. Cells (4×10^6 per mL) were treated with 50 μM α-TOS in the presence or absence of 100 mM DMPO. Analyses of DMPO spin-trapped adducts were performed with samples (200 μL) taken from the cell suspension and transferred into a quartz flat cell (Wilmad, Buena, CA). The cell was then placed into the cavity for EPR analyses at 293 K. The detection limit of the stable nitroxide (TEMPO) under identical conditions was ~50 nM. The time between removal of the sample, transfer to the flat cell, and tuning the spectrometer was <30 s. EPR spectra were obtained as an average of five scans (modulation frequency, 100 kHz; sweep time, 163 s). Microwave power, modulation amplitude, and scan range used for each analysis are as indicated in the figure legend. Hyperfine couplings were obtained by spectral simulation using WINSIM software (*43*) and are expressed in units of mT. Simulations were considered acceptable if they produced correlation factors of $R > 0.85$. Diethylenetriamine pentaacetic acid (DTPA; Sigma) (100 μM) was added to cell suspensions before exposure to α-TOS to avoid complications of Fenton-type chemistry.

Assessment of Sphingomyelin (SM) Metabolism and SMase Activity. The involvement of SM metabolism in α-TOS-induced apoptosis was estimated as published previously (*44*). Cells were metabolically labeled with [methyl-^{3}H]-choline (0.5 μCi/ml) and stimulated with α-TOS (50 μM) with or without Z-VAD-FMK (25 μM). At indicated times, cells were harvested and homogenized by sonication. Lipids were extracted from the lysates, and [^{3}H]choline-labeled SM quantified as described (*45*). Alternatively, SM and ceramide contents were determined by [9,10-^{3}H]palmitic acid labeling as previously reported (*45*). In short, [9,10-^{3}H]palmitic acid-labeled lipids were separated by this-layer chromatography and the radioactive lipids localized by radioscanning.

SMase activity was determined in cells exposed to α-TOS with or without Z-VAD-FMK (see above) as reported (*44*). An aliquot of cell lysate was combined with [choline-methyl-^{14}C]SM (1.2×10^5 dpm/assay), and the amount of liberated [methyl-^{14}C]choline was quantified by liquid scintillation counting (*44*).

Products formed during sphingomyelin hydrolysis were characterized by negative ion-spray liquid chromatography−mass spectroscopy (LC-MS) as described (*46*). In brief, 15 × 10^6 cells (0.5×10^6 per mL) were treated for 30, 60, or 90 min with 50 μM α-TOS or 40 ng/mL hrTRAIL, washed two times with PBS, and the pellet extracted as published earlier (*47*). Extracts were dried under a stream of argon and dissolved in 80 μL chloroform/methanol (1:2, v/v) prior to analysis. Lipids were analyzed by direct injection into the Esquire 3000 mass spectrometer (Bruker) using the flow of 9 μL/min. The electrospray probe was operated at a negative ion mode. The molecular ion (*m*/*z* 536) and chlorine adduct of C16 ceramide (*m*/*z* 572) were isolated and accumulated in the ion trap. For quantification, the sum of arithmetic mean of parallel measurements of both ions was used. Authentic C16 ceramide (Calbiochem) was used as a standard.

Cell Fractionation. Cells were fractionated into cytosolic, mitochondrial, and nuclear compartments according to the standard protocol using sequential centrifugation (*48*). Ml-1a, C19, and P2 cells, sensitive to the conventional method, were fractionated by cavitation (*32*).

Treatment with Bcl-2 Oligodeoxynucleotides (ODN). Bcl-2 antisense, reverse antisense or sense, phosphorothioate-modified ODNs (*49*) were synthesized (MWG-Biotech) and used as follows. Cells (0.5×10^6 per mL) were supplemented with 10 μM ODN or left untreated. After 18 h, aliquots for Bcl-2 immunoblotting were taken, and a second portion of ODN (10 μM) was added together with α-TOS. Aliquots for second Bcl-2 immunoblotting were taken 14 h later, and apoptosis assessed 12 h after α-TOS addition.

Transfections. The following plasmids were used: Bcl-2-EGFP, Bcl-x_L-EGFP, Bax-EGFP, and their carboxy terminal deletion mutants (*50*), cyt *c*-EGFP (*51*), pMito-RFP (red fluorescent protein; Clontech), dominant-negative (DN) caspase-9 (*52*), and cFLIP (*53*). Transfections were carried out essentially as described (*24*). In brief, cells at 50−70% confluence were supplemented with 5 μg DNA preincubated for 10 min with 10 μL LipofectAMINE (Gibco-Life Technologies) and 1 mL serum-free EMEM. After 1−2 h, cells were washed and supplemented with complete EMEM. After 24−36 h, cells were exposed to apoptosis inducers as indicated elsewhere. For apoptosis evaluation, cells were cotransfected with 4 μg of a functional gene-EGFP vector and 1 μg of the histone-EGFP vector or pRFP (*54*). Following treatment with apoptotic inducers, cells with green nuclei or red cytoplasm were scored using fluorescence microscope. Transfection efficacy was, routinely, 50−60%, as assessed by expression of EGFP or RFP.

Western Blotting. Whole cell lysates were separated by 15% SDS−PAGE and proteins transferred onto nitrocellulose membranes, which were blocked, incubated with antibodies against cyt *c*, caspase-9 (PharMingen), Bcl-2, AIF, or Bid (Santa Cruz) and incubated further with peroxidase-labeled secondary IgG. Blots were developed using the ECL kit (Amersham) and exposed to X-Omat AR film.

Immunofluorescence Microscopy. Suspension cells (0.25×10^6) were cytospun, while adherent cells were grown on cover slips, fixed, permeabilized, and incubated with antibodies against cyt *c* (PharMingen), AIF (Santa Cruz), or Smac/Diablo (Alexis). The cells were then incubated with secondary FITC- (Santa Cruz) or Alexa-488-conjugated IgG (Molecular Probes), mounted with Mowiol (Sigma) or Vectashield-DAPI (Victor Laboratories), and observed using a Leica DMRBE microscope.

Transmission Electron Microscopy. Cells (10^7) were grown in complete RPMI medium at 0.5×10^6 per mL, treated as indicated, spun down, fixed with 2% glutaraldehyde and post-fixed with 1% OsO_4, made up in isotone cacodylate buffer (pH 7.2; 300 mOsmol), dehydrated, and embedded in Epon-812. Ultrathin sections were cut, contrasted with uranyl acetate and lead citrate, and examined in a JEOL 1200 EX transmission electron microscope operated at 80 kV (*55*).

Statistics. Unless stated otherwise, the data shown are mean values ± SD of three independent experiments. The differences were considered significant when $P < 0.05$, as assessed by Student's t-test. The images shown are representative pictures derived from at least three independent experiments.

RESULTS

α-TOS Causes Morphological Changes Typical for Apoptosis. Recent reports suggested that apoptosis induced by α-TOS involves destabilization of intracellular organelles including mitochondria (*26*, *56*). This prompted us to investigate the early changes associated with α-TOS-triggered apoptosis and link them to downstream events. A typical feature shared by diverse modes of apoptosis is changes in (sub)cellular morphology, including that of mitochondria, as documented by transmission electron microscopy for Jurkat cells treated with α-TOS, anti-Fas IgM, or hrTRAIL (Figure 1). Although morphological changes typifying different stages of apoptosis are shown here, α-TOS-induced apoptosis was, in most respects, morphologically undistinguishable from that initiated by Fas or TRAIL.

Switching on of the SM Cycle and Radical Formation Are Early Events in α-TOS-Initiated Pro-Apoptotic Signaling. An important role in apoptosis modulation has been ascribed to SM metabolites, and SMase is often activated early in apoptosis. Table 1 reveals that α-TOS exposure led to a transient two-phase decrease in the level of SM in cells, and that the second phase was suppressed by the pan-caspase inhibitor Z-VAD-FMK. In contrary, SM hydrolysis occurred later in TRAIL-treated cells and was not inhibitable by Z-VAD-FMK. Concomitantly, treatment of the cells with α-TOS resulted in formation of ceramide with kinetics resembling that of SM hydrolysis, and this was correlated with activation of SMase (Table 1). Negative ion-spray LC-MS analysis of cells treated with both α-TOS and hrTRAIL revealed C16 ceramide as a major SM-derived metabolite. Importantly, LC-MS analysis showed that the kinetics of C16 ceramide formation reflected degradation of SM as well as activation of SMase (Figure 2, cf. Table 1). The potential role of SM metabolism in α-TOS-induced apoptosis was further supported by its partial suppression by desipramine, an inhibitor of acidic SMase (Table 2).

Formation of radicals may be an important event in α-TOS-induced apoptosis (*34*). Figure 3A reveals an early buildup of oxidative stress in α-TOS-exposed cells, while this was delayed in cells treated with anti-Fas IgM and hrTRAIL. Fas- and TRAIL-dependent ROS generation was suppressed by the pan-caspase inhibitor Z-VAD-FMK, but this was not observed for α-TOS. To confirm that the observed increase in fluorescence was due to oxidation of DCDF, we used as a negative control carboxy-DCDF, an analogue of DCDF insensitive to oxidation (Figure 3A, inset). The fact that we observed no changes in the fluorescence of carboxy-DCDF in cells exposed to α-TOS (Figure 3A, inset) suggests that changes in fluorescence of DCDF in cells exposed to α-TOS were largely due to oxidation of the probe. To confirm the role of oxidative stress in α-TOS-induced apoptosis, we pretreated Jurkat cells with NAC, α-TOH, mito-E, or mito-Q. Figure 3B shows that antioxidants suppressed both oxidative stress and apoptosis induction in α-TOS-exposed cells and that the mitochondrially targeted analogues were similarly protective at ~50-fold lower concentrations compared to α-TOH. These data also strongly advocate mitochondria as a source of radicals.

To obtain direct evidence for ROS formation in cells exposed to α-TOS, we employed EPR spectroscopy together with spin trapping (Figure 4). Treatment of cells with α-TOS for 1 h in the presence of DMPO generated a weak four-line spectrum super-posed on a broad multiplet absorption: these adducts were present for up to 5 h incubation (Figure 4A, B). Hyperfine couplings of the spin adduct exhibiting a sharp EPR signal were from single nitrogen (A^N) and hydrogen ($A^H{}_\beta$) atoms. Coupling constants $A^N \sim 1.51$ mT and $A^H{}_\beta \sim 1.46$ mT were determined by spectral simulation (not shown) and are consistent with the assignment of a hydroxyl radical adduct of DMPO (*57*). In contrast, the broad signal is likely due to the formation of an oxidation/breakdown product of DMPO that is also present in commercial sources of DMPO prior to purification (not shown). Comparison of the DMPO adduct obtained from the cell system with authentic DMPO-OH obtained from the reaction of DMPO and H_2O_2/Fe^{2+} indicates that the major radical species generated during α-TOS exposure of cells. Superoxide radical aducts of DMPO may be subsequently converted to DMPO-OH. Therefore, we cannot rule out the possibility that α-TOS exposure of cells increases superoxide production (Figure 4C) (*42*). Importantly, no radicals were detected in reaction mixtures containing cells alone, cells loaded with DMPO without α-TOS treatment, and DMPO alone as controls (Figure 4D−F). Although these experiments were performed with THP-1 cells, they are likely similar with Jurkat cells, as both cell lines exert similar kinetics of apoptosis when exposed to α-TOS (not shown). It needs to be pointed out, though, that these data do not exclude the possibility that some of the EPR-detected radicals are derived from a mitochondria-independent process. Notwithstanding, these results provide a direct evidence for generation of ROS in cells exposed to α-TOS and support the idea that radicals may be involved in early pro-apoptotic signaling.

A frequent result of increased intracellular oxidative stress is oxidation of GSH. We therefore investigated whether exposure of Jurkat cells to α-TOS would lead to a shift in the GSH-to-GSSG ratio. Table 3 shows a dramatic and early conversion of GSH to GSSG in cells exposed to α-TOS, whereas this was not observed for TRAIL. This further supports the notion of the role of ROS in early apoptosis induced by α-TOS.

Pro-Apoptotic Factors Are Mobilized in Cells Exposed to α-TOS. Mitochondrial destabilization is characterized by a decrease in $\Delta\Psi_m$. Figure 5A shows a drop in $\Delta\Psi_m$ in Jurkat cells exposed to α-TOS, while this was not prominent in cells treated with anti-Fas IgM. Co-treatment with Z-VAD-FMK partially inhibited these changes in anti-Fas IgM- but

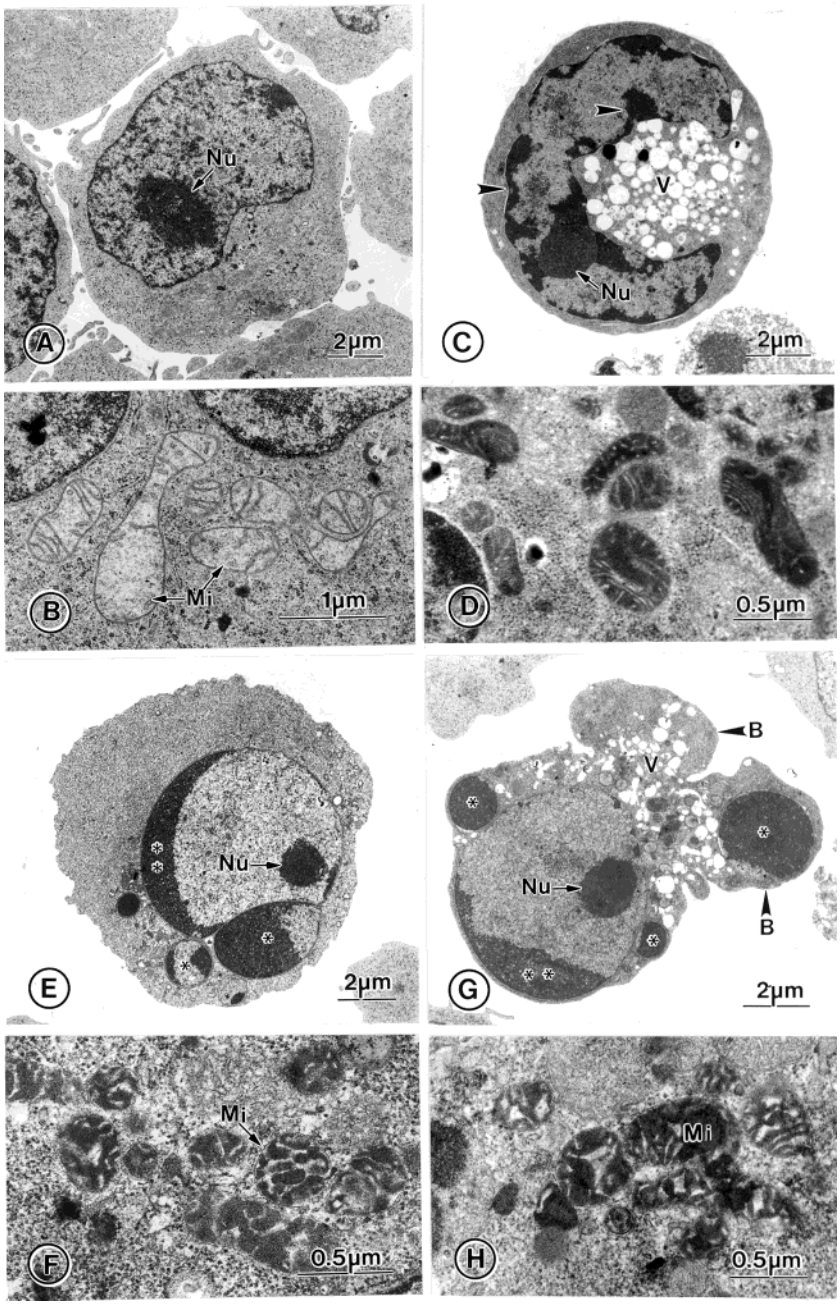

FIGURE 1: Ultrastructural alterations of Jurkat cells following exposure to various apoptosis-inducing agents. Compared to the control cells (A, B), 12 h treatment with either 50 μM α-TOS (C, D), 20 ng/mL anti-Fas IgM (E, F), or 40 ng/mL hrTRAIL (G, H) resulted in apoptosis of various stages. Characteristic ultrastructural features of the early apoptotic phase (C) are condensation and margination of the chromatin (arrowheads) and the appearance of numerous autophagic vacuoles (V). In a later stage (E, G), the condensed chromatin appears as crescent structures (**) on the inner nuclear membrane. As a result of nuclear membrane convolution and fragmentation, nuclear bodies (*) are formed (E, F). Finally, convolution of the cell membrane results in cellular blebs (B), which finally leads to fragmentation of the cell into apoptotic bodies (G). The various apoptotic treatments have transformed the orthodox mitochondria of the control cells (B) to the condensed conformation, which is characterized by the condensed matrix and either relatively normal (D) or swollen intercristal space (F, G).

not α-TOS-treated cells. Contrary to $\Delta\Psi_m$, Z-VAD-FMK suppressed activation of both caspase-3 and -6 in cells exposed to α-TOS (not shown).

Mitochondrial destabilization often leads to mobilization of pro-apoptotic factors such as cyt *c*, AIF, or Smac/Diablo. Figure 5B shows a loss of granulated pattern typical for cyt *c* in Jurkat cells exposed to α-TOS, which was not suppressed by Z-VAD-FMK. The diffuse pattern was partially suppressed in cells co-treated with Z-VAD-FMK and anti-Fas IgM. Immunoblotting of fractionated cells confirmed cytosolic translocation of cyt *c* but failed to show nuclear relocalization of AIF (Figure 5C).

In the adherent cell line MCF7-C3, we also observed cyt *c* relocalization during apoptosis induced by α-TOS (Figure 5D). MCF7-C3 cells treated with α-TOS showed diffuse pattern of cyt *c* as well as of AIF and Smac/Diablo, suggestive of relocalization of these pro-apoptotic factors from mitochondria (Figure 5E). Such changes were not observed in MCF7-C3 cells treated with hrTRAIL (not shown).

Caspase-9 Is Important for Post-Mitochondrial Events in α-TOS-Induced Apoptosis. To dissect initial caspase signaling in α-TOS and Fas/TRAIL apoptosis, we pretreated cells with the caspase-9 inhibitor Z-LEHD-FMK or the caspase-8

Table 1: Sphingomyelin Metabolism Is Switched on in α-TOS-Treated Cells[a]

time (min)	SM hydrolysis[b]				ceramide formation[c]		SMase activity[d]	
	α-TOS		hrTRAIL		α-TOS		α-TOS	
	−zVAD	+zVAD	−zVAD	+zVAD	−zVAD	+zVAD	−zVAD	+zVAD
10	1.0 ± 0.1	1.11 ± 0.04	n.d.	n.d.	n.d.	n.d.	n.d.	n.d.
15	0.83 ± 0.02*	0.87 ± 0.01*	1.04 ± 0.12	1.12 ± 0.06	n.d.	n.d.	1.6	1.6
30	0.89 ± 0.02*	0.88 ± 0.01*	1.14 ± 0.16	0.95 ± 0.04	1.1	0.9	1.4	1.3
45	0.79 ± 0.01*	0.81 ± 0.01*	1.04 ± 0.06	0.98 ± 0.07	1.3	1.35	1.6	1.25
60	1.08 ± 0.12	1.11 ± 0.12	0.78 ± 0.07*	0.83 ± 0.02*	1.08	0.88	1.5	1.2
90	0.77 ± 0.02*	1.07 ± 0.12	0.82 ± 0.01*	0.89 ± 0.06*	1.2	0.7	1.3	1.1
120	1.06 ± 0.11	1.05 ± 0.07	1.02 ± 0.06	0.97 ± 0.01	0.9	0.7	1.1	1.04

[a] Jurkat cells (0.5×10^6 per mL) were exposed to α-TOS (50 μM) or hrTRAIL (40 ng/mL) for the time indicated, analyzed for the level of SM and ceramide or Smase activity as detailed in Materials and Methods, and this was expressed as a change in SM level relative to untreated cells. [b] Data are derived from 3−4 independent experiments and are expressed as mean values ± S.D. The asterisk indicates the relative level of SM statistically different from that in nontreated cells with $P < 0.05$. n.d., not determined. [c] Data are mean values from one experiment performed in triplicate with S.D. less than 10%. Sphingomyelinase activity is expressed as the ratio of the activity of the treated sample and the unstimulated control. The specific activity of the control was 2.3 ± 0.4 nmol h^{-1} mg^{-1} protein.

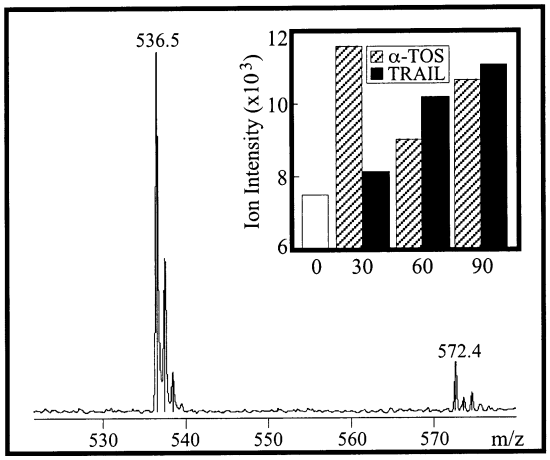

FIGURE 2: C16 ceramide is formed during α-TOS- and TRAIL-induced apoptosis. α-TOS activates the sphingomyelin pathway. Jurkat cells were exposed to α-TOS (50 μM) or hrTRAIL (40 ng/mL) for 30, 60, or 90 min and assessed for generation of C16 ceramide by negative ion-spray MS (inset). The data are average values of two analyses. Authentic C16 ceramide was used to obtain a standard MS spectrum, which was correlated with that obtained by analysis of treated. Note that the relative increase in the level of C16 ceramide corresponds to the loss of SM and formation of total ceramide and can be correlated with SMase activation as shown in Table 1.

Table 2: Desipiramine Inhibits α-TOS-Induced Apoptosis[a]

time (h)	apoptosis (%)[b]		
	Des	α-TOS	α-TOS + Des
0	10.5 ± 1.2	−	−
6	11.7 ± 2.1	23.5 ± 3.2	15.2 ± 1.8*
22	13.8 ± 1.9	90.5 ± 7.8	59.3 ± 6.2*

[a] Jurkat cells (0.5×10^6 per mL) were incubated with desipramine (Des; 5 μM), α-TOS (50 μM) or the two agents together for 6 or 22 h. [b] Apoptosis was assessed using the annexin V-FITC method and is expressed as % of annexin V-positive cells. The asterisk indicates differences in apoptosis level in samples treated with α-TOS + Des statistically different from those treated with α-TOS only with $P < 0.05$.

inhibitor Z-IETD-FMK. The caspase-9 inhibitor suppressed caspase-3 activation and PS externalization for α-TOS whereas these effects were less pronounced for both Fas and TRAIL, and the opposite was observed with the caspase-8 inhibitor (Figure 6A,B). Consistent with this, treatment of Jurkat cells with α-TOS resulted in activation of the initiator caspase-9, while this was not observed in case of Fas, at least in the earlier time points (Figure 6C,D).

Table 3: α-TOS Causes Conversion of GSH to GSSG[a]

time (h)	[GSSG]/[GSH]		
	control	α-TOS	hrTRAIL
0	0.11 ± 0.043	0.11 ± 0.037	0.11 ± 0.037
1	0.13 ± 0.033	0.27 ± 0.049*	0.08 ± 0.025
2	0. 1 ± 0.038	0.29 ± 0.08*	0.08 ± 0.047
6	0.12 ± 0.059	0.41 ± 0.04*	0.11 ± 0.052
12	0.09 ± 0.039	0.26 ± 0.062*	0.13 ± 0.034

[a] Jurkat cells (0.5×10^6 per mL) were treated with vehicle (control), α-TOS (50 μM), or hrTRAIN (40 ng/mL) and assessed for oxidized and reduced glutathione, as described in Materials and Methods, and their level expressed as a ratio of GSSG/GSH. Asterisk denotes statistical difference from the corresponding control values with $P < 0.05$.

As both α-TOS and TRAIL lead to activation of multiple effector caspases, we investigated the effect of these inducers on MCF7 (caspase-3-deficient) and MCF7-C3 (caspase-3-expressing) cells. As shown in Figure 6E, caspase-3-deficient cells showed lower susceptibility than their caspase-3-proficient counterparts when exposed to α-TOS as well as to hrTRAIL, suggestive of importance of caspase-3 for full apoptotic potential of the cells, unlike shown by a recent report indicating a compensatory use of alternative caspases (*58*).

Susceptibility to α-TOS Requires Fully Functional Mitochondria. Because mitochondria play an important role in α-TOS-induced apoptosis, we studied whether the absence of mtDNA affects susceptibility of cells to the agent, using ρ^0 cells (C19) derived from the Ml-1a cell line and their revertants (clone P2) (*32*). Figure 7 shows that C19 cells were more resistant to α-TOS than the parental cells and the P2 revertants. As cyt *c* is a major mediator of α-TOS apoptosis downstream from mitochondria, we studied its level in the Ml-1a, C19, and P2 cells and its relocalization during exposure to α-TOS. Figure 7C reveals that, unlike the parental cells and the revertants, C19 cells failed to relocalize cyt *c*, despite their higher total levels of cyt *c* compared to the other two cell lines (not shown). Therefore, the resistance of ρ^0 cells is linked to nonfunctional mitochondria rather than to lack of cyt *c*. Indeed, we also observed higher levels of cyt *c* in ρ^0 fibroblasts when compared to their normal counterparts (not shown).

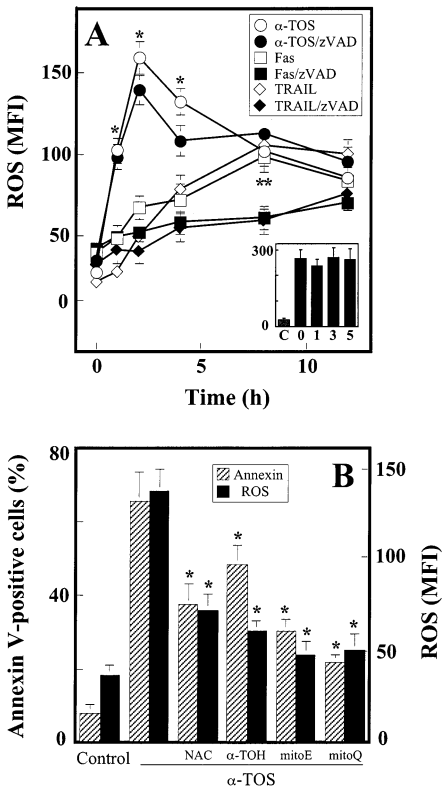

FIGURE 3: α-TOS induces generation of oxidative stress. (A) Jurkat cells were exposed to α-TOS (50 μM), anti-Fas IgM (20 ng/mL), or hrTRAIL (40 ng/mL) in the absence or presence of Z-VAD-FMK (25 μM), and generation of ROS was estimated by oxidation of DCDF, evaluated by FACS. The inset shows fluorescence in control cells, or in cells treated for 0, 1, 3, and 5 h with 50 μM α-TOS and incubated with carboxy-DCDF, an oxidation nonsensitive analogue. The symbol "*" indicates statistically different value for cells treated with α-TOS compared to cells treated with anti-Fas IgM or hrTRAIL, while the symbol "**" indicates statistically different values for cells treated with anti-Fas IgM or hrTRAIL alone compared to cells co-treated with zVAD. (B) Cells were pretreated with NAC (5 mM), α-TOH (50 μM), mito-E (2 μM), or mito-Q (1 μM) for 2 h and exposed to α-TOS (50 μM, 12 h), and apoptosis extent was evaluated by annexin V binding after 12 h and ROS generation using DCDF after 4 h. The symbol "*" indicates statistically significant differences ($P < 0.05$) in the values for cells treated with α-TOS alone and those co-treated with different antioxidants.

Bcl-2 Family Proteins Are Important for α-TOS-Induced Apoptosis. Release of cyt *c* from mitochondria into the cytosol is often modulated by the Bcl-2 family proteins. To assess the potential anti-apoptotic role of Bcl-2 in α-TOS-initiated cell death, we used gain- and loss-of-function Bcl-2 mutant strains of the H7 cell line. The loss-of-function cells were more susceptible and the gain-of-function cells more resistant to α-TOS, while these differences were less pronounced for TRAIL (Figure 8A). Further, Jurkat cells were sensitized to α-TOS, but less so to Fas, following downregulation of Bcl-2 by antisense ODN treatment (Figure 8B, C), as also supported by their susceptibility to α-TOS at concentrations sub-apoptotic for ODN-untreated cells (Figure 8B, inset).

We studied the role of Bcl-2 family proteins using MCF7-C3 cells transfected with fusion constructs harboring EGFP and the Bcl-2, Bcl-x_L, or Bax genes or their mutants lacking the mitochondrial-docking domain. Figure 8D shows that overexpression of both Bcl-2 and Bcl-x_L, but not ΔBcl-2 or

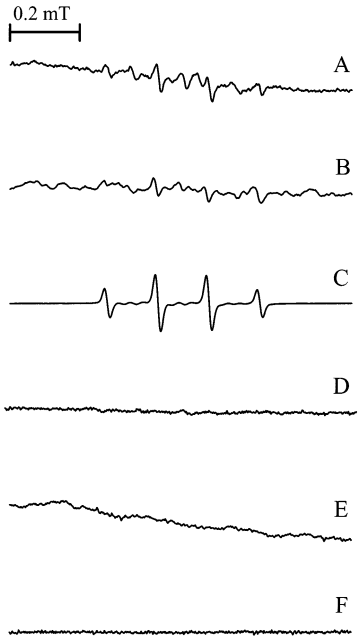

FIGURE 4: EPR spectroscopy reveals radical generation in cells treated with α-TOS. THP-1 cells (4×10^6 per mL) were preincubated with 100 mM DMPO and exposed to α-TOS (50 μM) for 1 (A) or 5 h (B). A reference EPR spectrum was obtained by reacting DMPO with H_2O_2 in the presence of Cu^{2+} (C). EPR spectra are shown of the control cell (D), cells loaded with DMPO and incubated in the absence of α-TOS (E), and cells with α-TOS in the absence of DMPO (F).

ΔBcl-x_L, suppressed α-TOS-induced apoptosis. Overexpression of Bax, but not ΔBax, sensitized cells to α-TOS. Similar trend was found when these transfectants were exposed to TRAIL (Figure 8E). Expression of EGFP-tagged Bcl-2 and Bcl-x_L, but not their deletion mutants, revealed punctuated patterns of fluorescence, while this was observed for Bax, but not ΔBax, upon cell exposure to α-TOS as well as to TRAIL (not shown), suggesting mitochondrial translocation of Bax during apoptosis.

Proximal Signaling Is Involved in Receptor- but not in α-TOS-Initiated Apoptosis. We next investigated the effect of proximal versus distal signaling in α-TOS-induced apoptosis. Figure 9A shows that Fas-DN Jurkat cells were resistant to anti-Fas IgM but not α-TOS. Moreover, Fas-induced apoptosis was inhibited in wild-type cells with neutralizing anti-Fas IgG (not shown). Jurkat cells overexpressing CrmA exerted resistance to both Fas and TRAIL but not to α-TOS (Figure 9B). To further delineate the differences in pro-apoptotic signaling by α-TOS and TRAIL, we transfected MCF7-C3 cells with DN-caspase-9 or cFLIP and exposed them to the two apoptogens. Results in Figure 9C show that cells overexpressing DN-caspase-9 were protected from α-TOS but not from TRAIL, while the opposite occurred in cFLIP-overexpressing cells.

α-TOS Cooperates with Anti-Fas IgM in Apoptosis Induction. Given the fact that the pro-apoptosis pathways induced by α-TOS and by the immunological agents partially differ yet converge at the level of the effector caspases, we tested a potential combinatorial effect of α-TOS and anti-Fas IgM. Figure 10A shows that while the extent of apoptosis in the cells treated with 20 μM α-TOS or 5 ng/mL anti-Fas IgM did not significantly differ from control cells, exposure of the cells to a combination of these agents yielded 50−60%

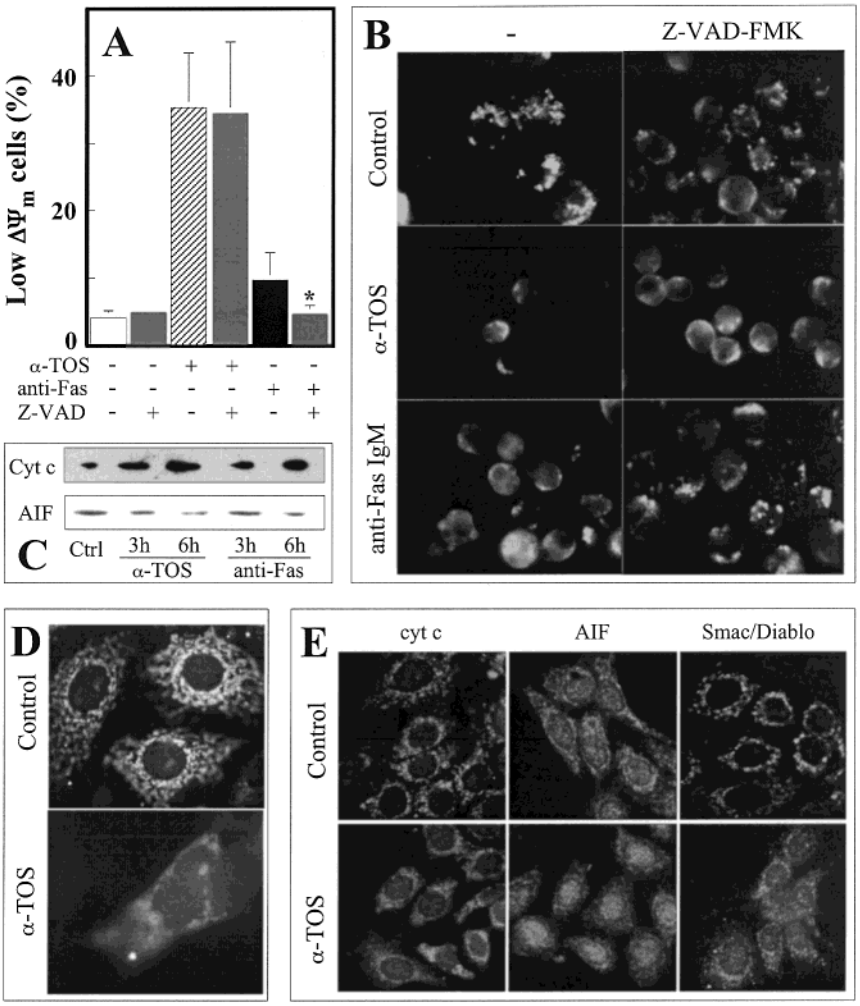

FIGURE 5: α-TOS causes mitochondrial destabilization and mobilization of pro-apoptotic factors. (A) Jurkat cells were exposed to α-TOS (50 μM) or anti-Fas IgM (20 ng/mL) for 6 h in the absence or presence of Z-VAD-FMK (25 μM) and assessed for $\Delta\Psi_m$ by FACS following staining with JC-1. The symbol "*" indicates statistically significant differences ($P < 0.05$) in the values for cells treated with anti-Fas IgM alone and cells co-treated with zVAD. (B) Jurkat cells were exposed to 50 μM α-TOS or 20 ng/mL anti-Fas IgM for 9 h unless indicated otherwise. The cells were then cytospun, stained with anti-cyt *c* IgG, and observed in fluorescence microscope or (C) fractionated, lysed, and probed by immunoblotting for the level of cyt *c* (cytosolic fraction) or AIF (nuclear fraction). (D) MCF7-C3 cells were cotransfected with pCyt *c*-EGFP and pMito-RFP and exposed to α-TOS for 12 h. (E) MCF7-C3 cells were exposed to 50 μM α-TOS for 12 h and immunostained for cyt *c*, AIF, and Smac/Diablo, followed by a secondary FITC- or Alexa-488-conjugated IgG.

apoptosis. This enhanced effect was confirmed on the level of caspase-3 activity increase (Figure 10B). Both PS externalization and caspase-3 activation in the co-treatment experiments were suppressed by preincubation with the neutralizing anti-Fas IgG (Figure 10).

DISCUSSION

In this report we present evidence that mitochondria play a central role in α-TOS-induced apoptosis, that mitochondrial destabilization is crucial for caspase activation, and that the pro-apoptotic pathways in α-TOS-induced and receptor-mediated apoptosis converge at the level of effector caspases. This notion is supported by several lines of evidence: (i) treatment of Jurkat cells with α-TOS leads to switching on of the sphingomyelin cycle and rapid generation of ROS, followed by cyt *c* and Smac/Diablo release, and activation of caspase-9, −3 and −6; (ii) activation of caspases, but not generation of ROS, decrease of $\Delta\Psi_m$, and release of pro-apoptotic factors, can be suppressed by caspase inhibitors; (iii) Bcl-2 overexpression protects from α-TOS while its down-regulation sensitizes cells toward the agent; (iv) mtDNA deficiency results in lower susceptibility to α-TOS including lack of cyt *c* relocalization; (v) caspase-9 is dispensable for Fas or TRAIL but crucial for α-TOS-induced apoptosis.

Mitochondria have been implicated in apoptosis induction by α-TOS (*23*, *28*, *34*, *56*), but the up- and downstream events as well as its regulation have not been investigated in detail. The first event in cells exposed to α-TOS observed was switching on of SM metabolism; i.e., there was a significant loss of SM and formation of ceramide in as little as 15 min (cf. Table 1). It is difficult to explain the two phases of SM hydrolysis in cells exposed to α-TOS and suppression of the latter by a pan-caspase inhibitor, as activation of caspases appears to be a later event. This finding is consistent, though, with a report showing biphasic and early formation of ceramide in Fas-exposed Jurkat cells (*59*), while others reported a delayed ceramide generation in a similar system (*46*). Contrary to α-TOS, only the second phase of SM decrease was observed in cells exposed to TRAIL, pointing to differences in early events in pro-apoptotic signaling of α-TOS and TRAIL. Similarly, as

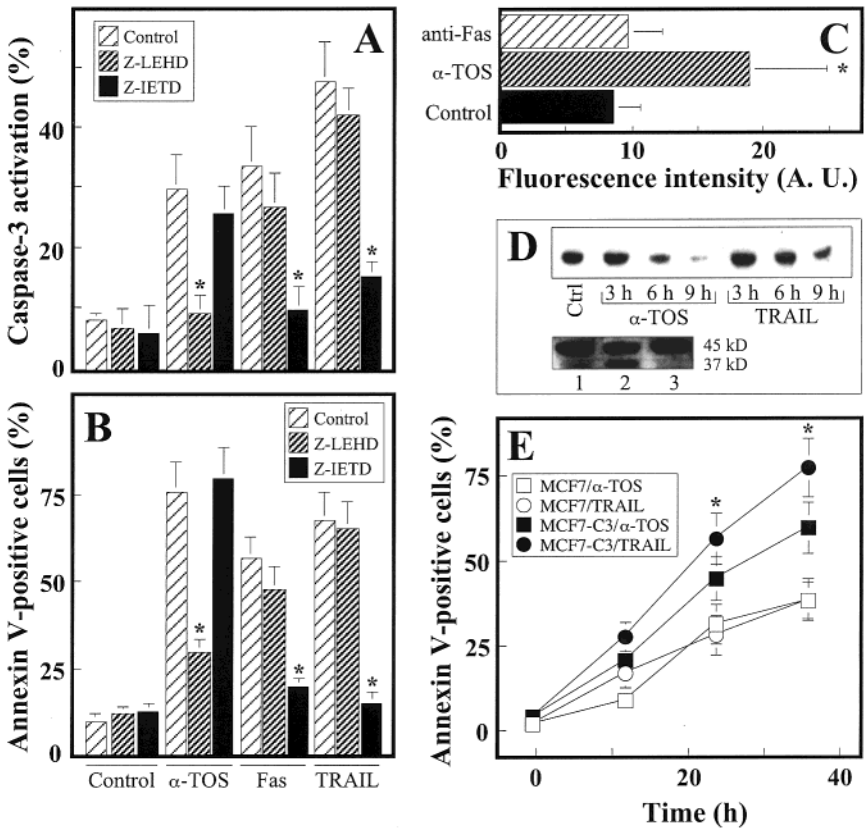

FIGURE 6: Caspase 9 is activated in α-TOS-induced apoptosis. Jurkat cells were exposed to α-TOS (50 μM), anti-Fas IgM (20 ng/mL), or hrTRAIL (40 ng/mL) in the absence or presence (25 μM) of the caspase-9 inhibitor Z-LEHD-FMK or the caspase-8 inhibitor Z-IETD-FMK and assessed for caspase-3 activation using the anti-activated caspase-3 IgG (A) and for PS externalization by annexin V binding (B). The symbol "*" indicates statistically significant differences ($P < 0.05$) in the values for cells treated with the inducer of apoptosis alone and those co-treated with caspase inhibitors. (C) Jurkat cells were exposed to α-TOS or anti-Fas IgG (see above) for 6 h, and caspase-9 activity was analyzed. The symbol "*" indicates statistically different values for control cells and cells treated with α-TOS. The cells were also assessed for the level of pro-caspase-9 by Western blotting following treatment with the two agents for the periods indicated (D). Bottom panel in D shows cleavage of pro-caspase-9 to caspase-9 in control cells (1) and cells treated for 6 h with α-TOS (2) and anti-Fas IgM (3). (E) MCF7 and MCF7-C3 cells were exposed to α-TOS (50 μM) or hrTRAIL (40 ng/mL) for the time indicated and assessed for PS externalization by annexin V binding. The symbol "*" indicates statistically significant differences ($P < 0.05$) in the values for MCF7-C3 and MCF7 cells.

shown for Jurkat cells treated with Fas (*46*), we identified C16 ceramide as a major metabolite of SM in both α-TOS- and TRAIL-exposed Jurkat cells. Moreover, LC-MS analysis revealed that the kinetics of C16 ceramide formation and the increase in its relative amount could be correlated with that of SM loss, total ceramide generation and SMase activation (cf. Figure 2 and Table 1).

We have recently observed that α-TOS causes lysosomal instability (*23*) with early leak of lysosomal constituents into the cytosol (*60*). While not measured here, it is plausible that translocation of lysosomal SMase can contribute to SM metabolism, although the exact role of the acidic and neutral SMase is unclear (*61*). This is supported by an experiment, which showed that desipramine, an inhibitor of acidic SMase (*62*), partially suppressed α-TOS-induced apoptosis (cf. Table 2). One of the pathways involved in α-TOS apoptosis is deregulation of the protein phosphatase 2A (PP2A)/protein kinase C (PKC) pathway; i.e., α-TOS induces activation of PP2A that, in turn, inactivates PKC (*24*). May and co-workers showed that generation of ceramide leads to PP2A activation with ensuing PKCα inactivation that, consequently, results in dephosphorylation of bcl-2 at Ser 70, whereby lowering the level of mitochondrially docked Bcl-2 (*20*, *21*, *31*). Therefore, α-TOS-induced generation of ceramide may be a link between the VE analogue and activation of PP2A, although the possibility that α-TOS activates PP2A directly cannot be ruled out (*24*, *63*). This link is supported by higher resistance to apoptosis of the Bcl-2 gain-of-function and higher susceptibility to death of the Bcl-2 loss-of-function cells exposed to α-TOS (cf. Figure 8A).

We and others have observed that inactivation of PKCα is not always sufficient to induce apoptosis and, rather, that this process can amplify other signaling pathways (*24*, *64*). In case of α-TOS, the presence of the succinyl moiety is essential for the apoptosis-inducing activity of the agent (*24*, *60*). This is based on experiments using β-TOS, an analogue with high pro-apoptotic efficacy but lacking the PKC inhibitory activity, whose apoptogenic potential resides solely with the succinyl moiety (*24*, *63*). α-TOS acts as a stressor to which the cell responds by generation of ROS (*65*, *66*), a process that may involve NADPH-dependent oxidase (*41*, *67*). ROS can also be generated by mitochondria as a response to ceramide (*68*), or to sphingosine, a product of ceramide catabolism (*69*). A contributory role of ROS in α-TOS-induced apoptosis is supported by experiments in which radical scavengers suppressed cell death (cf. Figure 3). We confirmed ROS generation in α-TOS-exposed cells directly by EPR spectroscopy. This approach allowed us to detect a hydroxyl-like radical; it is possible that, in line with a recent report (*67*), superoxide is formed in α-TOS-stressed

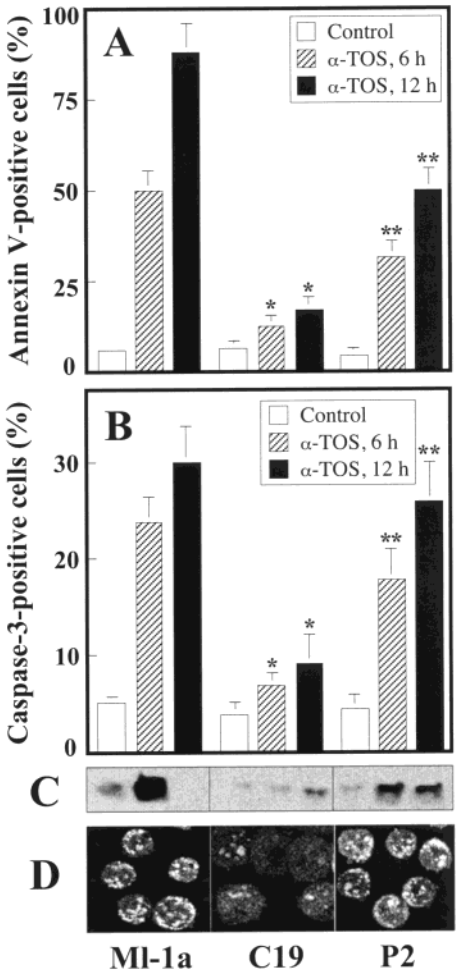

FIGURE 7: mtDNA-deficient cells are resistant to α-TOS. Ml-1a cells and their clones, the mtDNA-deficient C19 and the revertant P2 cells, were exposed to α-TOS (50 μM) for 6 and 12 h and assessed for apoptosis (A) and caspase-3 activation (B). α-TOS-treated cells were also fractionated and the cytosolic fraction immunoprobed for cyt *c* (C). Deficiency in mtDNA was evaluated by EtBr staining (D). The symbol "*" indicates statistically significant differences ($P < 0.05$) in the values for α-TOS-treated Ml-1a cells and their C19 counterparts, while the symbol "**" indicates statistically significant differences ($P < 0.05$) in the values for α-TOS-treated P2 and C19 clones.

cells that can be, at least partially, converted to hydroxyl radicals whose accumulation was observed in DMPO-loaded cells (cf. Figure 4). We also observed conversion of GSH to its oxidized form (cf. Table 3), a frequent result of increased intracellular oxidative stress and a potentiating event in apoptosis (*70*), and another piece of evidence for a change in the cellular redox tone in early stages of α-TOS-induced cell death signaling.

Although the site of ROS generation in cells exposed to α-TOS is unclear, our data point to mitochondria as their source and, probably, also their target. This is supported in particular by suppression of apoptosis by mitochondrially targeted antioxidants, viz mito-E and mito-Q. These compounds contain at the end of their aliphatic side chain a positively charged triphenylphosphonium group, which transports them to mitochondria, so that the charged group resides within the mitochondrial matrix while its quinone function is on the surface of the mitochondrial inner membrane. Consequently, the ratio of these agents localized in mitochondria and cytosol is ~1000:1 (*36*). In fact, these mitochondrially targeted agents were comparably protective against α-TOS at concentrations ~50-fold lower than α-TOH (cf. Figure 3).

Earlier reports suggested that α-TOS caused release of pro-apoptotic factors from mitochondria into the cytosol, such as that of cyt *c* in HL-60 cells (*56*). As α-TOS leads to release of this mediator also in Jurkat and MCF7 cells (this report), cyt *c* relocalization appears to be a unifying principle in pro-apoptotic signaling of the VE analogue and ranks it to drugs whose main pathway involves mitochondrial destabilization. Similarly as shown for HL-60 cells (*56*), α-TOS induced dissipation of $\Delta\Psi_m$ in Jurkat cells (cf. Figure 5) in a cyclosporin A-independent way (not shown). This is suggestive of opening of the mitochondrial permeability transition pore (*5*, *6*). We have also observed that mitochondrial destabilization in α-TOS-induced apoptosis led to relocalization of Smac/Diablo, a protein that forms a complex in the cytosol with the IAP family members, which prevents their association with and thereby suppression of caspase activity (*11*, *12*). Interestingly, a negative regulation of apoptosis has been shown between SM metabolism and regulation of IAP activity in Jurkat cells, as sphingosine-1-phosphate suppressed Smac/Diablo as well as cyt *c* relocalization (*71*). We have observed that dimethylsphingosine, an inhibitor of sphingosine kinase, potentiated α-TOS-induced apoptosis in Jurkat cells (not shown). Although we did not study the causal relationship between Smac/Diablo translocation and apoptosis induction, it is possible that this pathway, by suppressing the caspase-inhibitory activity of the IAPs, maximizes sensitivity of cells to α-TOS. We have also observed nuclear relocalization of AIF (*8*) in MCF7-C3 but not Jurkat cells (cf. Figure 5E), suggestive of a cell-type specific process. Notwithstanding, these results give further support for mitochondrial role in α-TOS-induced apoptosis.

Relocalization of mitochondrial factors, in particular that of cyt *c*, links mitochondrial destabilization to downstream events, of which activation of caspase-9 appears crucial for a variety of apoptogens (*4*, *5*). This is also the case for α-TOS, as documented by activation of caspase-9 in Jurkat cells exposed to the agent, by inhibition of α-TOS-induced apoptosis by a caspase-9 inhibitor, and by transfecting epithelial cancer cells with DN-caspase-9 (cf. Figures 6 and 9). On the other hand, caspase-9 inhibitors failed to significantly suppress apoptosis induced in Jurkat cells by both anti-Fas IgM and hrTRAIL (cf. Figure 6). This is rather surprising as Jurkat cells have been classified as the so-called "type II" cells, in which the level of caspase-8 is too low to activate directly the effector caspases but sufficient to cleave Bid to its pro-apoptotic form (*14*). Similar to Jurkat cells, MCF7 cells transfected with DN-caspase-9 were susceptible to both immunological apoptogens (cf. Figure 9) (*14*). These data are consistent with recent reports that overexpression of DN-caspase-9 is permissive for caspase-3 activation and full susceptibility to apoptosis induction by TRAIL in the HCT116 cells (*28*, *72*). Our findings appear consistent with the notion of some researchers that the type I and type II classification is not always plausible (*2*), or that there are differences in pro-apoptotic signaling even within the same cell line. Collectively, as shown in this communication for Jurkat and MCF7 cells and in an earlier report for endothelial cells (*37*), α-TOS acts as a typical inducer of apoptosis using

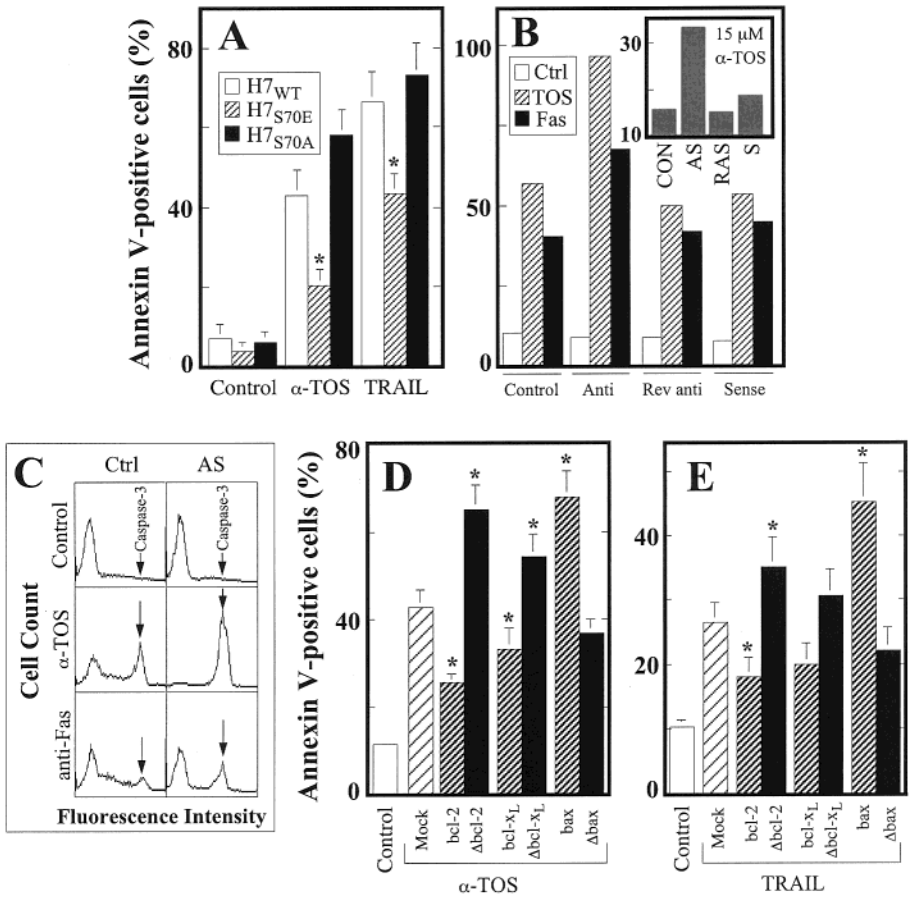

FIGURE 8: Bcl-2 family proteins play an important role in α-TOS-initiated apoptosis. (A) Wild-type (WT), Bcl-2 loss-of-function (S70A), and Bcl-2 gain-of-function (S70E) H7 cells were exposed to α-TOS (50 μM) or hrTRAIL (40 ng/mL) for 12 h, and the extent of apoptosis was assessed. The symbol "*" indicates significantly different values for treated $H7_{S70E}$ and $H7_{WT}$ cells. Jurkat cells were pretreated with anti-sense (AS), sense (S), or reverse anti-sense (RAS) bcl-2 ODN, exposed to α-TOS (30 μM, 12 h), and assessed for apoptosis using annexin V-FITC (B) and caspase-3 activation based on binding an antibody recognizing activated caspase-3 (the population of cells with activated caspase-3 is indicated by arrow) (C). The inset in (B) shows apoptosis in ODN-treated cells exposed for 12 h to 15 μM α-TOS. MCF7-C3 cells were transfected with pBcl-2-EGFP, pBcl-x_L-EGFP, and pBax-EGFP, or their deletion (Δ) mutants. The cells were then exposed to α-TOS (50 μM, 24 h) (D) or hrTRAIL (40 ng/mL) (E), and apoptosis extent was evaluated. The symbol "*" indicates statistically significant differences ($P < 0.05$) in the values for mock-transfected cells and those transfected with various wild-type genes or their deletion mutants.

the mitochondrial pathway. Its major downstream signaling consists of formation of the apoptosome (*37*), following cyt *c* relocalization, and activation of caspase-9 followed by activation of the effector caspases, a pathway shared by a variety of pharmacological inducers of apoptosis (*4*, *73*).

Several studies reported that cells with impaired mitochondria are more resistant to apoptosis induced by as diverse apoptogens as TNF-α (*32*, *74*) and staurosporine (*75*), while others observed no discernible differences (*76*). The so-called ρ^0 phenotype (mtDNA deficiency) was prepared by long-term treatment of cells with EtBr, and such cells were devoid of proteins coded for by mtDNA but not proteins derived from nuclear DNA. One possible explanation for higher resistance of ρ^0 cells was that they lack oxidative phosphorylation and therefore energy necessary for operating the complex apoptotic machinery (*75*). We have observed that the mtDNA-deficient C19 cells derived from Ml-1a cells were resistant in PS externalization and caspase-3 activation when challenged with α-TOS compared to the parental cells and the revertants prepared by fusion of the C19 cells with platelets (*32*) (cf. Figure 7). That the importance of normal levels of mtDNA-derived proteins for efficient apoptotic response to α-TOS may be a general phenomenon is suggested by resistance to α-TOS of ρ^0 HeLa cells (D. S. Ucker, personal communication). Curiously, several types of ρ^0 cells feature higher levels of mitochondria-associated proteins including cyt *c*. In some (*32*, *74*) but not all apoptosis-resistant ρ^0 cells (*73*), there was a lack in cyt *c* release. We failed to observed cyt *c* translocation in the C19 cells treated with α-TOS (cf. Figure 7), despite higher mitochondrial level of the protein (not shown). This is consistent with recent report showing the importance of respiratory activity for cyt *c* relocalization (*74*). Finally, it is possible that rho-0 cells are resistant to apoptosis due to expression of survival factors, as they feature constitutively activated nuclear factor-κB (Higuchi, M., Manna, S. K., Sasaki, R., and Aggarwal, B. B. (2002) *Antioxid. Redox Signaling 4*, 945−955). Collectively, these findings stress the importance of functional mitochondria in apoptosis induced by α-TOS, and strongly suggest cyt *c* relocalization as a major post-mitochondrial event, relaying mitochondrial injury to activation of the caspase cascade.

Multiple studies have shown that mitochondrial destabilization with ensuing downstream events can be regulated by Bcl-2 family proteins. Of these, we studied Bcl-2 and Bcl-x_L, whose anti-apoptotic activity can be antagonized by

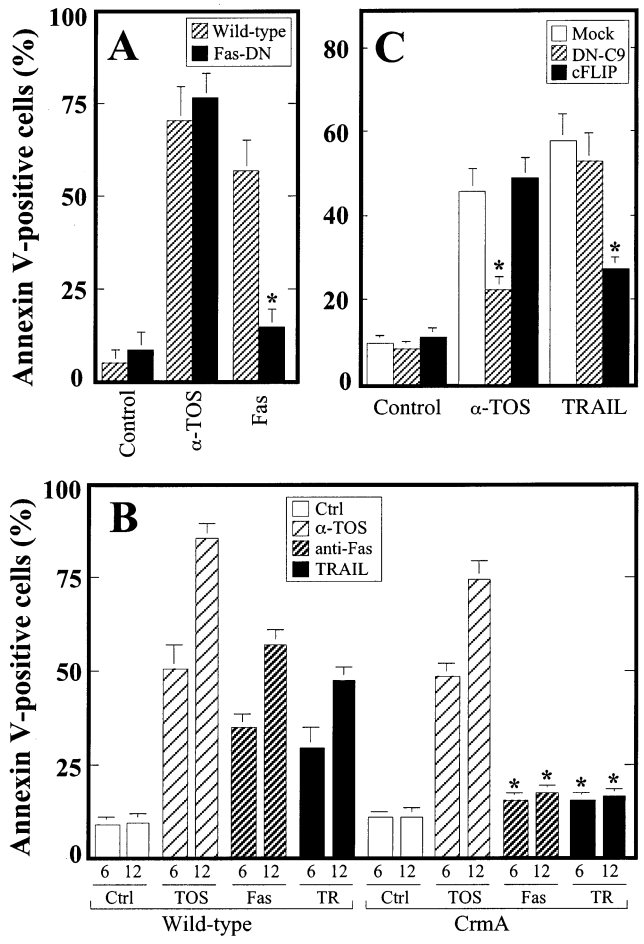

FIGURE 9: Proximal signaling is involved in receptor- but not in α-TOS-induced apoptosis. (A) Wild-type and Fas-DN Jurkat cells were exposed to α-TOS (50 μM) or anti-Fas IgM (20 ng/mL) for 12 h, and the extent of apoptosis was evaluated. (B) Wild-type and CrmA-transfected Jurkat cells were exposed to α-TOS (50 μM), anti-Fas IgM (20 ng/mL) or hrTRAIL (TR; 40 ng/mL) for 6 or 12 h, and apoptosis extent was evaluated. (C) MCF7-C3 cells were transfected with either DN-caspase-9 (DN-C9) or cFLIP, exposed to α-TOS (50 μM) or hrTRAIL IgM (40 ng/mL) for 24 h, and the extent of apoptosis was evaluated. The symbol "*" indicates statistically significant differences ($P < 0.05$) in the values for treated wild-type cells and their transfected counterparts.

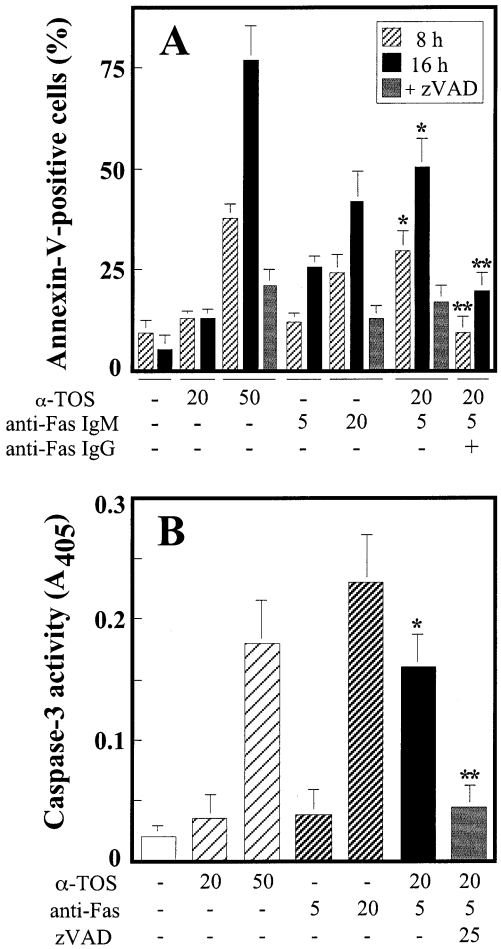

FIGURE 10: α-TOS cooperates with anti-Fas IgM in apoptosis induction. Jurkat cells were treated with the vehicle, α-TOS (μM), or anti-Fas IgM (ng/mL) in the absence or presence of anti-Fas IgG (100 ng/mL), and assessed for apoptosis (A; 8 or 16 h treatment) and caspase-3 activation (B; 8 h treatment). Where indicated, cells were co-treated with Z-VAD-FMK (25 μM) for 8 h. The symbol "*" indicates statistically significant differences ($P < 0.05$) in the values for cells treated with sub-apoptotic levels of α-TOS or anti-Fas IgM alone, and cells were co-treated with the two inducers. The symbol "**" indicates statistically significant differences ($P < 0.05$) in the values for cells treated with sub-apoptotic levels of α-TOS and anti-Fas IgM in combination, and the cells co-treated with anti-Fas IgG (A) or zVAD (B).

Bax (*16*). A crucial role of Bcl-2 in stabilizing mitochondria against α-TOS-induced damage follows from the following findings: (i) Bcl-2 loss-of-function cells were more and the Bcl-2 gain-of-function cells less resistant to α-TOS; (ii) down-regulation of Bcl-2 by antisense ODN treatment rendered cells more susceptible to α-TOS; and (iii) overexpression of Bcl-2 and Bcl-x_L, but not of their deletion mutant lacking the mitochondrial-docking sequence, conferred resistant to α-TOS. One way by which Bcl-2 can be destabilized is mitochondrial translocation of Bax that can form heterodimers and thereby inactivate Bcl-2, or oligomerize and form pores in the outer mitochondrial membrane (*77*). We have observed association of Bax with mitochondria as a response of cells to α-TOS, and this was abolished when cells were transfected with a Bax mutant that lacks the mitochondrial-docking sequence (cf. Figure 8). Moreover, overexpression of Bax, but not its deletion mutant, sensitized cells to α-TOS.

Bcl-2 family proteins are classified according to the number of the Bcl-2 homology (BH) domains. The anti-apoptotic proteins contain BH1-4 domains, which is the case for Bcl-2. Another protein comprising these domains is Bcl-x_L, which appears to act similarly as does Bcl-2. Unlike Bcl-2 that resides not only in mitochondria but also in the endoplasmatic reticulum (*78*), Bcl-x_L is exclusively mitochondrial (*16*, *49*). Consistent with various chemical inducers of apoptosis, overexpression of the wild-type but not the deletion mutant of Bcl-x_L rendered cells resistant to α-TOS (cf. Figure 8).

The BH3-only protein Bid is cleaved in certain types of apoptosis, such as shown for the type II cells, where cleavage of Bid to its truncated, pro-apoptotic form tBid by the initiator caspase-8 occurs rather than direct activation of the effector caspases (*14*, *16*). Generally, tBid can be expected to relay receptor engagement, such as shown in some reports for Fas-initiated apoptosis, to mitochondrial events (*14*, *16*, *79*) and has been suggested to promote activation of pro-apoptotic proteins such as Bax (*49*, *80*). While cleavage of Bid has been observed in HL-60 cells exposed to α-TOS

(*56*), we did not observe this in α-TOS-treated Jurkat cells (not shown). Collectively, these results strongly suggest that the main pro-apoptotic signaling pathway of α-TOS, at least in our model, proceeds directly via mitochondria, at which level it can be regulated both positively and negatively by multiple members of the Bcl-2 family.

As discussed earlier, blocking the mitochondrial pathway by transfection with DN-caspase-9 rendered the cells more resistant to α-TOS, while shutting down the receptor pathway by overexpression of cFLIP or CrmA was protective against immunological apoptogens (cf. Figure 9). Therefore, combination of these agents using different signaling pathways as their major mode of apoptosis induction may show a cooperative effect by virtue of maximizing the pro-apoptotic potential of the cell. We have observed this in Jurkat cells exposed to combined α-TOS and anti-Fas IgM at sub-apoptotic levels (cf. Figure 10). This is reminiscent of similar cooperative effects of α-TOS and TRAIL in apoptosis induction and suppression of experimental colon cancer (*28*). Moreover, α-TOS has been shown to sensitize breast cancer cells to Fas killing by regulating surface expression of Fas (*81*).

We believe that the major mode of action of α-TOS is mitochondrial destabilization with ensuing downstream events, while other reports suggested regulation of additional signaling pathways, including the c-jun (*27*, *82*) or TGF-β pathway (*83*). It is possible that both mitochondrial destabilization and signaling via transcriptional regulation are operational in α-TOS-induced apoptosis. The extent of contribution of the major modes of action to the overall pro-apoptotic efficacy of α-TOS may vary depending on the cell type and on the concentration of the agent, and requires further investigations.

On the basis of these results, we propose a mechanism of α-TOS-induced apoptosis, in which mitochondria play a central role. As depicted in Scheme 1, α-TOS translocates to membranous structures of the cell, where it can activate SMase, which, in turn, leads to generation of ceramide that can destabilize mitochondria. SMase activation and mitochondrial destabilization can be also promoted by lysosomal destabilization and ROS generation. These events result in opening of the transition pores and release of pro-apoptotic factors such as cyt *c*, Smac/Diablo, and AIF. Mitochondrial destabilization can be regulated by the Bcl-2 family proteins. Formation of the apoptosome, composed of cyt *c*, Apaf-1, and pro-caspase-9, leads to activation of the initiator caspase-9, followed by activation of the effector caspase-3 and −6. Smac/Diablo may be involved by suppressing the anti-apoptotic activity of the IAP family members, inhibitors of caspases, while AIF can transmit mitochondrial injury directly to nuclear apoptotic events. On the other hand, receptor-mediated apoptosis involves proximal transmembrane signaling, leading to recruitment and activation of the initiator caspase-8, which, either directly and/or via destabilization of mitochondria, activates effector caspases.

We conclude that α-TOS is a powerful inducer of apoptosis in multiple cell types, whose major pathway utilizes the mitochondrial route, that seem to transmit downstream the early responses to the agent. As this semisynthetic VE analogue has low toxicity toward normal cells or tissues, can overcome resistance of cancer cells to antitumor drugs due to mutations in tumor suppressor genes, and cooperates in vitro and in vivo with immunological inducers of apoptosis, it is a promising candidate for an anticancer agent of therapeutic interest. This intriguing concept is furthered by the notion according to which apoptosis-signaling pathways including the mitochondrial events offer a powerful target for anticancer therapy yet to be utilized in its full potential (*84*, *85*).

Scheme 1: Possible Pathways Involved in α-TOS-Induced Apoptosis in Jurkat Cells and Their Comparison with Pathways Operational in Receptor-Mediated Apoptosis[a]

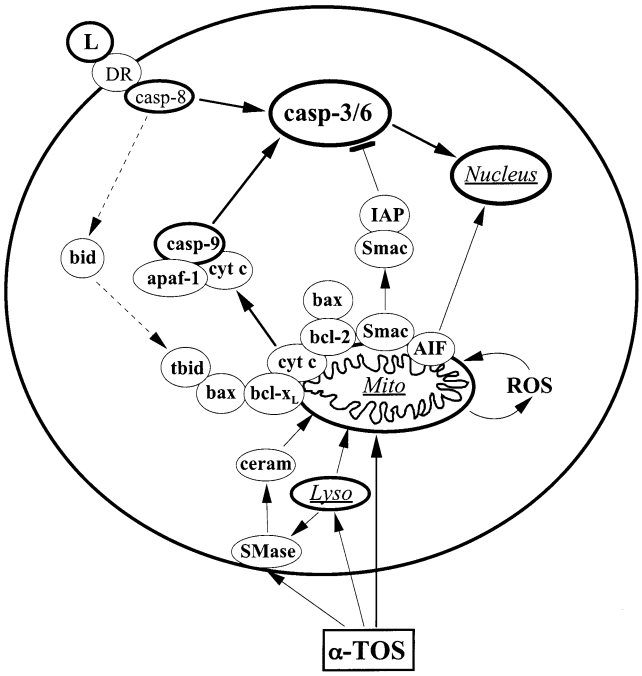

[a] α-TOS translocates to the cell where it activates acidic and/or neutral SMase, possibly (but not exclusively) by destabilization of lysosomes, giving rise to the lipid second messenger ceramide. α-TOS directly and/or via ceramide formation destabilizes the mitochondrial membrane, and this process may be amplified by generation of ROS. Mitochondrial destabilization, likely promoted also by leakage of lysosomal proteases, leads to cytosolic relocalization of proapoptotic factors like cyt *c*, Smac/Diablo or AIF, that can by regulated by the Bcl-2 family proteins. Cyt *c* forms a ternary complex with Apaf-1 and pro-caspase-9, resulting in activation of the initiator caspase-9 that, in turn, leads to activation of the effector caspases. Smac/Diablo may amplify this process by suppressing the caspase-inhibitory activity of the IAP family proteins, while AIF is supposed to transmit mitochondrial destabilization to nuclear apoptotic events. In receptor-mediated signaling, a ligand (L) interacts with its cognate death receptor (DR), leading to recruitment and activation of the initiator pro-caspase-8 that, either directly and/or via destabilization of mitochondria, activates effector caspases

ACKNOWLEDGMENT

The authors wish to thank Drs. S. J. Korsmeyer for Bcl-2-overexpressing, M. E. Peter for Fas-DN, and S. Gamen for CrmA-overexpressing Jurkat cells, W.S. May for the H7-derived Bcl-2 gain- and loss-of-function cell lines, M. Jämtallää for the caspase-3 MCF7 transfectant, R. J. Youle for the EGFP fusion constructs of Bcl-2, Bcl-x_L, and Bax and their deletion mutants, A. L. Nieminen for pCyt *c*-EGFP, C. Vincenz for the DN caspase-9 plasmid, J. Tschopp for pFLIP, M. P. Murphy for mito-E and mito-Q, and F. V. Pallardo for help with the glutathione assays. Technical assistance of A. M. S. Austarheim, M. F. Frisach, T. F.

Guldbrandsen, U. Johansson, R. Neuzilova, and M. Zhao is highly acknowledged. This work forms a part of doctoral thesis of T. W.

REFERENCES

1. Fadeel, B., Orrenius, S., and Zhivotovsky, B. (1999) *Biochem. Biophys. Res. Commun. 266*, 699−717.
2. Strasser, A., O'Connor, L., and Dixit, V. M. (2000) *Annu. Rev. Biochem. 69*, 217−245.
3. Ashkenazi, A., and Dixit, V. M. (1998) *Science 281*, 1305−1308.
4. Sun, X. M., MacFarlane, M., Zhuang, J., Wolf, B. B., Green, D. R., and Cohen, G. M. (1999) *J. Biol. Chem. 274*, 5053−5060.
5. Wolf, B. B., and Green, D. R. (1999) *J. Biol. Chem. 274*, 20049−20052.
6. Mignotte, B., and Vayssiere, J. L. (1998) *Eur. J. Biochem. 252*, 1−15.
7. Zamzami, N., Marchetti, P., Castedo, M., Decaudin, D., Macho, A., Hirsch, T., Susin, S. A., Petit, P. X., Mignotte, B., and Kroemer, G. (1995) *J. Exp. Med. 182*, 367−377.
8. Susin, S. A., Lorenzo, H. K., Zamzami, N., Marzo, I., Snow, B. E., Brothers, G. M., Mangion, J., Jacotot, E., Costantini, P., Loeffler, M., Larochette, N., Goodlett, D. R., Aebersold, R., Siderovski, D. P., Penninger, J. M., and Kroemer, G. (1999) *Nature 397*, 441−446.
9. Kluck, R. M., Bossy-Wetzel, E., Green, D. R., and Newmeyer, D. D. (1997) *Science 275*, 1132−1136.
10. Luo, X., Budihardjo, I., Zou, H., Slaughter, C., and Wang, X. (1998) *Cell 94*, 481−490.
11. Chai, J., Du, C., Wu, J. W., Kyin, S., Wang, X., and Shi, Y. (2000) *Nature 406*, 855−862.
12. Verhagen, A. M., Ekert, P. G., Pakusch, M., Silke, J., Connolly, L. M., Reid, G. E., Moritz, R. L., Simpson, R. J., and Vaux, D. L. (2000) *Cell 102*, 43−53.
13. Li, P., Nijhawan, D., Budihardjo, I., Srinivasula, S. M., Ahmad, M., Alnemri, E. S., and Wang, X. (1997) *Cell 91*, 479−489.
14. Scaffidi, C., Fulda, S., Srinivasan, A., Friesen, C., Li, F., Tomaselli, K. J., Debatin, K. M., Krammer, P. H., and Peter, M. E. (1998) *EMBO J. 17*, 1675−1687.
15. Ferrari, D., Stepczynska, A., Los, M., Wesselborg, S., and Schulze-Osthoff, K. (1998) *J. Exp. Med. 188*, 979−984.
16. Adams, J. M., and Cory, S. (1998) *Science 281*, 1322−1326.
17. Hockenbery, D. M., Oltvai, Z. N., Yin, X. M., Milliman, C. L., and Korsmeyer, S. J. (1993) *Cell 75*, 241−251.
18. Susin, S. A., Zamzami, N., Castedo, M., Hirsch, T., Marchetti, P., Macho, A., Daugas, E., Geuskens, M., and Kroemer, G. (1996) *J. Exp. Med. 184*, 1331−1341.
19. Dimmeler, S., Breitschopf, K., Haendeler, J. and Zeiher, A. M. (1999) *J. Exp. Med. 189*, 1815−1822.
20. Ito, T., Deng, X., Carr, B. K., and May, W. S. (1997) *J. Biol. Chem. 272*, 11671−11673.
21. Ruvolo, P. P., Deng, X., Carr, B. K., and May, W. S. (1998) *J. Biol. Chem. 273*, 25436−25442.
22. Cheng, E. H., Kirsch, D. G., Clem, R. J., Ravi, R., Kastan, M. B., Bedi, A., Ueno, K., and Hardwick, J. M. (1997) *Science 278*, 1966−1968.
23. Neuzil, J., Svensson, I., Weber, T., Weber, C., and Brunk, U. T. (1999) *FEBS Lett. 445*, 295−300.
24. Neuzil, J., Weber, T., Schröder, A., Lu, M., Ostermann, G., Gellert, N., Mayne, G. C., Olejnicka, O., Negre-Salvayre, A., Sticha, M., Coffey, R. J., and Weber, C. (2001) *FASEB J. 15*, 403−415.
25. Chinery, R., J. A. Brockman, M. O. Peeler, Y. Shyr, R. D. Beauchamp, and R. J. Coffey. (1997) *Nat. Med. 3*, 1233−1241.
26. Neuzil, J., Weber, T., Gellert, N., and Weber, C. (2001) *Br. J. Cancer 84*, 87−89.
27. Qian, M., Kralova, J., Yu, W., Bose, H. R., Dvorak, M., Sanders, B. G., and Kline, K. (1997) *Oncogene 15*, 223−230.
28. Weber, T., Lu, M., Andera, L., Lahm, H., Gellert, N., Fariss, M. W., Korinek, V., Sattler, W., Ucker, D. S., Terman, A., Schröder, A., Erl, W., Brunk, U. T., Coffey, R. J., Weber, C., and Neuzil, J. (2002) *Clin. Cancer Res. 8*, 863−869.
29. Chinnaiyan, A. M., Tepper, C. G., Seldin, M. F., O'Rourke, K., Kischkel, F. C., Hellbardt, S., Krammer, P. H., Peter, M. E., and Dixit, V. M. (1996) *J. Biol. Chem. 271*, 4961−4965.
30. Gamen, S., Anel, A., Perez-Galan, P., Lasierra, P., Johnson, D., A. Pineiro, and Naval, J. (2000) *Exp. Cell Res. 258*, 223−235.
31. Ruvolo, P. P., Deng, X., Carr, B. K., and May, W. S. (1999) *J. Biol. Chem. 274*, 20296−20300.
32. Higuchi, M., B. B. Aggarwal, and T. Yeh. (1997) *J. Clin. Invest. 99*, 1751−1758.
33. Mathiasen, I. S., Lademann, U., and Jäättelä, M. (1999) *Cancer Res. 59*, 4848−4856.
34. Alleva, R., Tomasetti, M., Andera, L., Gellert, N., Borghi, B., Weber, C., Murphy, M. P., and Neuzil, J. (2001) *FEBS Lett. 503*, 46−50.
35. Smith, R. A., Porteous, C. M., Coulter, C. V., and Murphy, M. P. (1999) *Eur. J. Biochem*. 263, 709−716.
36. Kelso, G. F., Porteous, C. M., Coulter, C. V., Hughes, G., Porteous, W. K., Ledgerwood, E. C., Smith, R. A., and Murphy, M. P. (2001) *J. Biol. Chem.* 276, 4588−4596.
37. Neuzil, J., Schröder, A., von Hundelshausen, P., Zernecke, A., Weber, T., Gellert, N., and Weber, C. (2001) *Biochemistry 40*, 4686−4692.
38. Reed, D. J., Babson, J. R., Beatty, P. W., Brodie, A. E., Ellis, W. W., and Potter, D. W. (1980) *Anal. Biochem. 106*, 55−62.
39. Asensi, M., Sastre, J., Pallardo, F. V., Estrela, J. M., and Viña, J. (1994) *Methods Enzymol. 234*, 367−371.
40. Arakaki, N., Kajihara, T., Arakaki, R., Ohnishi, T., Kazi, J. A., Nakashima, H., and Daikuhara, Y. *J. Biol. Chem. 274*, 13541−13546.
41. Kotake, Y., Reineke, L. A., Tanigawa, T., and Koshida, H. (1994) *Free Radical Biol. Med. 17*, 215−223.
42. Rosen, G. M., Brtigan, B. E., Halpern, H. G., and Pou, S. (1999) *Free Radicals: Biology and Detection by Spin Trapping*, Oxford University Press, Oxford.
43. Duling, D. R. (1994) *J. Magn. Reson. 104B*, 105−110.
44. Auge, N., Andrieu, N., Negre-Salvayre, A., Thiers, J. C., Levade, T., and Salvayre, R. (1996) *J. Biol. Chem. 271*, 19251−19255.
45. Auge, N., Escargueil-Blanc. I., Lajoie-Mazenc, I., Suc, I., Andrieu-Abadie, N., Pieraggi, M. T., Chatelut, M., Thiers, J. C., Jaffrezou, J. P., Laurent, G., Levade, T., Negre-Salvayre, A., and Salvayre, R. (1998) *J. Biol. Chem. 273*, 12893−12900.
46. Thomas, R. L., Matsko, C. M., Lotze, M. T., and Amoscato, A. A. (1999) *J. Biol. Chem. 274*, 30580−30588.
47. Ritov, V. B., Banni, S., Yalowich, J. C., Day, B. W., Claycamp, H. G., Corongiu, F. P., and Kagan, V. E. (1996) *Biochim. Biophys. Acta 1283*, 127−150.
48. Bossy-Wetzel, E., and Green, D. R. (2000) *Methods Enzymol. 322*, 235−242.
49. Reed, J. C., Stein, C., Subasinghe, C., Haldar, S., Croce, C. M., Yum, S., and Cohen, J. (1990) *Cancer Res. 50*, 6565−6570.
50. Wolter, K. G., Hsu, Y. T., Smith, C. L., Nechushtan, A., Xi, X. G., and Youle, R. J. (1997) *J. Cell Biol. 139*, 1281−1292.
51. Heiskanen, K. M., Bhat, M. B., Wang, H. W., Ma, J., and Nieminen, A. L. (1999) *J. Biol. Chem. 274*, 5654−5658.
52. Song, Q., Kuang, Y., Dixit, V. M., and Vincenz, C. (1999) *EMBO J. 18*, 167−178.
53. Schneider, P., Thome, M., Burns, K., Bodmer, J. L., Hofmann, K., Kataoka, T., Holler, N., and Tschopp, J. (1997) *Immunity 7*, 831−836.
54. Harvey, J. K., Lukovic, D., and Ucker, D. S. (2000) *J. Cell Biol. 148*, 59−72.
55. Brunk, U. T., Zhang, H, Dalen, H., and Öllinger, K. (1995). *Free Radical Biol. Med. 19*, 813−822.
56. Yamamoto, S., Tamai, H., Ishisaka, R., Kanno, T., Arita, K., Kobuchi, H., and Utsumi, K. (2000) *Free Radical Res. 33*, 407−418.
57. Sargent, F. P., and Gardy, E. M. (1976) *Can. J. Chem. 54*, 275−279.
58. Zheng, T. S., Hunot, S., Kuida, K., Momoi, T., Srinivasan, A., Nicholson, D. W., Lazebnik, Y., and Flavell, R. A. (2000) *Nat. Med. 6*, 1241−1247.
59. Cuvillier, O., Edsall, L., and Spiegel, S.(2000) *J. Biol. Chem. 275*, 15691−15700.
60. Neuzil, J., Zhao, M., Ostermann, G., Sticha, M., Gellert, N., Weber, C., Eaton, J. W., and Brunk, U. T. (2002) *Biochem. J. 362*, 709−715.
61. Bezombes, C., Segui, B., Cuvillier, O., Bruno, A. P., Uro-Coste, E., Gouaze, V., Andrieu-Abadie, N., Carpentier, S., Laurent, G., Salvayre, R., Jaffrezou, J. P., and Levade, T. (2001) *FASEB J. 15*, 297−299.
62. Strelow, A., Bernardo, K., Adam-Klages, S., Linke, T., Sandhoff, K., Kronke, M., and Adam, D. (2000) *J. Exp. Med. 192*, 601−612.
63. Ricciarelli, R., Tasinato, A., Clement, S., Ozer, N. K., Boscoboinik, D., and Azzi, A. (1998) *Biochem. J. 334*, 243−249.

64. Benimetskaya, L., Miller, P., Benimetsky, S., Maciaszek, A., Guga, P., Beaucage, S. L., Wilk, A., Grajkowski, A., Halperin, A. L., and Stein, C. A. (2001) *Mol. Pharmacol. 60*, 1296−1307.
65. Kogure, K., Morita, M., Nakashima, S., Hama, S., Tokumura, A., and Fukuzawa, K. (2001) *Biochim. Biophys. Acta 1528*, 25−30.
66. Ottino, P., and Duncan, J. R. (1997) *Free Radical Biol. Med. 22*, 1145−1151.
67. Hiraoka, W., Vazquez, N., Nievez-Neira, W., Chanock, S. J., and Pommier, Y. (1998) *J. Clin. Invest. 102*, 1961−1968.
68. Quillet-Mary, A., Jaffrezou, J. P., Mansat, V., Bordier, C., Naval, J., and Laurent, G. (1997) *J. Biol. Chem. 272*, 21388−21395.
69. Kågedal, K., Zhao, M., Svensson, I., and Brunk U. T. (2001) *Biochem. J. 359*, 335−343.
70. Dai, J., Weinberg, R. S., Waxman, S., and Jing, Y. (1999) *Blood 93*, 268−277.
71. Cuvillier, O., and Levade, T. (2001) *Blood 98*, 2828−2836.
72. Deng, Y., Lin, Y., and Wu, X. (2002) *Genes. Dev. 16*, 33−45.
73. Luetjens, C. M., Kogel, D., Reimertz, C., Dussmann, H., Renz, A., Schulze-Osthoff, K., Nieminen, A. L., Poppe, M., and Prehn, J. H. (2001) *Mol. Pharmacol. 60*, 1008−1019.
74. Nishimura, G., Proske, R. J., Doyama, H., and Higuchi, M. (2001) *FEBS Lett. 505*, 399−404.
75. Dey, R., and Moraes, C. T. (2000) *J. Biol. Chem. 275*, 7087−7094.
76. Jiang, S., Cai, J., Wallace, D. C., and Jones, D. P. (1999) *J. Biol. Chem. 274*, 29905−29911.
77. Kroemer, G., and Reed, J. C. (2000) *Nat. Med. 6*, 513−519.
78. Rudner, J., Lepple-Wienhues, A., Budach, W., Berschauer, J., Friedrich, B., Wesselborg, S., Schulze-Oshoff, K., and Belka, C. (2001) *J. Cell Sci. 114*, 4161−4172.
79. Yin, X. M., Wang, K., Gross, A., Zhao, Y., Zinkel, S., Klocke, B., Roth, K. A., and Korsmeyer, S. J. (1999) *Nature 400*, 886−891.
80. Eskes, R., Desagher, S., Antonsson, B., and Martinou, J. C. (2000) *Mol. Cell Biol. 20*, 929−935.
81. Yu, W., Israel, K., Liao, Q. Y., Aldaz, C. M., Sanders, B. G., and Kline, K. (1999) *Cancer Res. 59*, 953−961.
82. Yu, W., Liao, Q. Y., Hantash, F. M., Sanders, B. G., and Kline, K. (2001) *Cancer Res. 61*, 6569−6576.
83. Turley, J. M., Funakoshi, S., Ruscetti, F. W., Kasper, J., Murphy, W. J., Longo, D. L., and Birchenall-Roberts, M. C. (1995) *Cell Growth Differ. 6*, 655−663.
84. Costantini, P., Jacotot, E., Decaudin, D., and Kroemer, G. (2000) *J. Natl. Cancer Inst. 92*, 1042−1053.
85. Martinou, J. C., and Green, D. R. (2001) *Nat. Rev. Mol. Cell Biol. 2*, 63−67.

BI020527J